JVI Journals.ASM.org

Reovirus Uses Multiple Endocytic Pathways for Cell Entry

Wade L. Schulz, Amelia K. Haj, and Leslie A. Schiff

Department of Microbiology, University of Minnesota, Minneapolis, Minnesota, USA

Entry of reovirus virions has been well studied in several tissue culture systems. After attachment to junctional adhesion molecule A (JAM-A), virions undergo clathrin-mediated endocytosis followed by proteolytic disassembly of the capsid and penetration to the cytoplasm. However, during *in vivo* infection of the intestinal tract, and likely in the tumor microenvironment, capsid proteolysis (uncoating) is initiated extracellularly. We used multiple approaches to determine if uncoated reovirus particles, called intermediate subviral particles (ISVPs), enter cells by directly penetrating the limiting membrane or if they take advantage of endocytic pathways to establish productive infection. We found that entry and infection by reovirus ISVPs was inhibited by dynasore, an inhibitor of dynamin-dependent endocytosis, as well as by genistein and dominant-negative caveolin-1, which block caveolar endocytosis. Inhibition of caveolar endocytosis also reduced infection by reovirus virions. Extraction of membrane cholesterol with methyl-β-cyclodextrin inhibited infection by virions but had no effect when infection was initiated with ISVPs. We found this pathway to be independent of both clathrin and caveolin. Together, these data suggest that reovirus virions can use both dynamin-dependent and dynamin-independent endocytic pathways during cell entry, and they reveal that reovirus ISVPs can take advantage of caveolar endocytosis to establish productive infection.

To establish infection, viruses must bypass the limiting membrane either at the cell surface or through an intracellular compartment, such as the endosome. Enveloped viruses achieve this through membrane fusion mediated by envelope glycoproteins (26). Viral membrane fusion can be triggered by receptor interactions at the plasma membrane or specific conditions within the endosome (27). For example, the fusogenic activity of some envelope glycoproteins, such as the dengue virus glycoprotein E and the influenza virus hemagglutinin (HA) protein, is triggered by acid-dependent conformational changes (27). Nonenveloped viruses are unable to take advantage of membrane fusion to enter cells and instead must disrupt or form pores in the limiting membrane. These processes may also be triggered by exposure to specific stimuli, such as low vesicular pH, proteases, or receptor interactions (83).

Reovirus is a nonenveloped, double-stranded RNA virus in the family *Reoviridae* that commonly infects humans but is rarely pathogenic in adults (79). The observation that reovirus replicates preferentially in transformed cells has led to its development as a human cancer therapy (2, 15). It is likely that a number of virus and host determinants contribute to reovirus' oncolytic potential. Early studies proposed a model in which mutations in Ras inhibit antiviral protein kinase R (PKR) signaling and activate other signal transduction pathways to promote viral protein synthesis and apoptosis in reovirus-infected transformed cells (76). More recent work from our laboratory and others revealed that efficient cell entry of reovirus particles into transformed cells is a major determinant of its oncolytic potential (2, 47, 71).

The molecular details of reovirus entry have been best characterized in L929 mouse fibroblasts. In this cell line, entry is initiated by interactions between virions and the cellular receptor junctional adhesion molecule A (JAM-A), followed by the activation of β1 integrins and uptake of viral particles through clathrin-mediated endocytosis (6, 39, 43, 44). Within vesicles of the endocytic compartment, the outermost capsid protein, σ3, is removed by proteolysis and the membrane penetration protein μ1 is exposed, generating an intermediate subviral particle (ISVP) (10, 37, 78). During oral infection *in vivo*, secreted pancreatic serine proteases in the intestinal tract remove σ3 extracellularly to form ISVPs (8, 9). ISVPs may also be formed extracellularly during oncolytic therapy, as tumor microenvironments are often characterized by a high concentration of secreted proteases (50, 75, 87).

Virions and ISVPs have distinct protein compositions and structures that may affect the mechanism used to enter host cells. Although clathrin-mediated endocytosis plays a role during infection by virions, studies have shown that this pathway is dispensable for infection by ISVPs (44). In addition, μ1, which is exposed on ISVPs, can cause membrane damage and chromium release when cells are infected at high multiplicities of infection (MOIs) (41, 89). This has led to the suggestion that ISVPs enter cells by direct membrane penetration. However, ISVPs have been detected within endocytic vesicles of infected cells (3, 78), leaving open the possibility that ISVPs require endocytosis to establish productive infection. In addition, many viruses are now known to take advantage of multiple endocytic pathways to enter cells (16, 49, 62). While it has been established that reovirus virions use clathrin-mediated endocytosis for cell entry (44), the importance of other pathways, such as caveolar and lipid raft-mediated endocytosis, is currently unknown (12, 18, 21, 52, 67). This led us to investigate the role of clathrin-independent endocytosis during infection by reovirus virions and ISVPs. We found that two different chemical agents which disrupt caveolar endocytosis inhibited particle uptake and replication of both virions and ISVPs. Experiments using dominant-negative caveolin-1 confirmed the role of caveolar endocytosis in infection by virions and ISVPs, and delayed-addition experiments revealed that inhibition of this

Received 17 July 2012 **Accepted** 4 September 2012
Published ahead of print 12 September 2012
Address correspondence to Leslie A. Schiff, schif002@umn.edu.

doi:10.1128/JVI.01861-12

pathway affected an early step of the viral life cycle. We also discovered that infection by virions was inhibited when cells were depleted of membrane cholesterol, but this effect was not observed when infections were initiated with ISVPs. These results provide some of the first evidence that reovirus ISVPs use endocytosis to productively infect host cells and that virions take advantage of multiple endocytic pathways to initiate infection.

MATERIALS AND METHODS

Cells and viruses. Murine L929 fibroblasts were maintained in suspension culture as previously described (78). A549 and 293 cells were maintained in RPMI medium (Gibco) supplemented to contain 10% fetal calf serum (Sigma), 50 U of penicillin/ml, 50 mg/ml streptomycin, and 2 mM glutamine.

Reovirus serotype 1 Lang (T1L) is a laboratory stock. Stocks were prepared by passage in L929 cells and purification as previously described (22). Briefly, virions were purified by CsCl density gradient centrifugation from extracts of cells infected with third-passage cell lysate stocks. Bands corresponding to the density of reovirus were collected and extensively dialyzed against virion dialysis buffer (3 M NaCl, 200 mM $MgCl_2$, 200 mM Tris, pH 7.5). Reovirus ISVPs were generated by incubating 1×10^{13} reovirus particles/ml with 200 μg/ml chymotrypsin in virion dialysis buffer at 32°C for 30 min. Reactions were terminated using 1 mM phenylmethylsulfonyl fluoride (PMSF), and the particle concentration was calculated using the equivalence of 1 U of optical density at 260 nm to 2.1×10^{12} particles. Viral titer was determined by plaque assay on L929 cells as described elsewhere (84).

Confocal imaging. A549 cells were plated in 8-well CultureSlides (BD Falcon) at a density of 7×10^4 cells/well. Twenty-four hours after plating, cells were treated with vehicle or inhibitor as described above and equilibrated at 4°C for 30 min. To image particle uptake, reovirus virions or ISVPs in gelatin (gel) saline were adsorbed at a concentration of 1×10^5 particles/cell at 4°C. After 1 h, warm medium with or without inhibitor was added to the cells. At 10 min postinfection (mpi), samples were fixed in 1.6% formaldehyde, permeabilized with 0.2% Triton X-100, and stained with Texas Red-labeled phalloidin (Invitrogen). Reovirus particles were detected using rabbit antiserum raised against reovirus T1L (Barbara Sherry, North Carolina State University) and DyLight 488-labeled donkey anti-rabbit antibodies (Jackson ImmunoResearch). To analyze the uptake of control ligands, Alexa Fluor 488-labeled transferrin (10 μg/ml; Invitrogen) or fluorescein isothiocyanate (FITC)-labeled cholera toxin subunit B (10 μg/ml; Sigma) in gel saline was adsorbed to cells at 4°C. After 1 h, warm medium with vehicle or inhibitor was added to the cells, and they were fixed 30 min later with 1.6% formaldehyde. Coverslips were mounted using Vectashield HardSet with 4′,6-diamidino-2-phenylindole (DAPI) (Vector Laboratories).

Analysis of viral growth. Cells were treated with 100 μM dynasore in dimethylsulfoxide (DMSO) (Sigma), 200 μM genistein in DMSO (Sigma), or 5 mM methyl-β-cyclodextrin (MβCD) in water (Sigma) for 1.5 h and then infected with reovirus T1L virions or ISVPs at an MOI of 3. After 1 h of adsorption at 4°C, cells were concentrated by low-speed centrifugation, resuspended in fresh medium, and added to dram vials (2×10^5 cells/vial) containing 1 ml of cold medium with vehicle or inhibitor. Cells were placed in a 37°C CO_2 incubator and subjected to three cycles of freezing and thawing at various times postinfection. Viral yields were determined by plaque assay on L929 cells as previously described (84).

Reovirus cell-binding assay. L929 cells were incubated at a concentration of 2×10^6 cells/ml with vehicle or inhibitor for 1.5 h at 37°C. Reovirus particles were then adsorbed at a concentration of 1×10^5 particles/cell at 4°C for 1 h. Cells were washed with phosphate-buffered saline (PBS), collected by low-speed centrifugation, and fixed in 1.6% formaldehyde. Viral particles were detected with rabbit antiserum raised against reovirus T1L and counterstained with allophycocyanin (APC)-conjugated anti-rabbit antibodies (Jackson ImmunoResearch). Viral binding was assessed by flow cytometry using an LSR II flow cytometer (BD Biosciences) and analyzed with the FlowJo analysis software (Treestar).

Cell viability assay. L929 cells were plated in 6-well trays, and medium containing vehicle or inhibitor was added for 24 h. Monolayers were detached using Cellstripper (Cellgro), and cells were stained with annexin V-FITC and propidium iodide (PI) using the TACS apoptosis detection kit (Trevigen). Viability was quantified by flow cytometry using an LSR II flow cytometer, and data were analyzed using the FlowJo analysis software.

Expression of dominant-negative caveolin-1. A plasmid expressing dominant-negative caveolin-1 (DN-cav1) with the Y14F mutation (25) and the empty control vector (pEGFP-N1) were obtained from Mark McNiven (Mayo Institute). 293 cells were plated in 6-well trays and transfected with pEGFP-N1 control vector or DN-cav1 using Lipofectamine 2000 (Invitrogen) at a DNA (μg)-to-Lipofectamine 2000 (μl) ratio of 1:2.5. Twenty-four hours posttransfection, cells were infected with reovirus T1L at an MOI of 20. Monolayers were detached with Cellstripper at 24 h postinfection (hpi), and cell suspensions were fixed with 1.6% formaldehyde. Fixed cells were washed with PBS, permeabilized with 0.2% Triton X-100, and analyzed for the presence of reovirus antigens using rabbit antiserum directed against the reovirus nonstructural protein μNS (Max Nibert, Harvard) and APC-labeled secondary antibody. Reovirus-infected cells were quantified by flow cytometry on an LSR II flow cytometer and analyzed with the FlowJo analysis software.

Immunoblot analysis of reovirus infection. Cell lysates were generated from L929 cells infected with reovirus at an MOI of 15. Lysates from the equivalent of 1×10^6 cells were run on a sodium dodecyl sulfate (SDS)-10% polyacrylamide gel and transferred to nitrocellulose. Membranes were blocked overnight in Tris-buffered saline-0.05% Tween (TBST) containing 10% nonfat dry milk. Expression of the reovirus nonstructural protein μNS was detected using rabbit antiserum, and β-actin expression was detected with a mouse monoclonal antibody (Santa Cruz Biotechnology). Membranes were washed with TBST and incubated with horseradish peroxidase-conjugated anti-rabbit IgG and anti-mouse IgG (GE Healthcare). Bound antibody was detected by treating the membranes with enhanced chemiluminescence detection reagents (Amersham). μNS expression relative to β-actin and an untreated control was calculated using ImageJ analysis software.

Statistical analysis. Mean values for triplicate samples are shown from representative growth experiments; error bars indicate the standard errors of the means. For ligand uptake and dominant-negative caveolin-1 experiments, mean values for at least triplicate samples were compared using a paired (normalized) or unpaired (nonnormalized) Student's *t* tests. *P* values of <0.05 were considered statistically significant.

RESULTS

Reovirus ISVPs are internalized by dynamin-dependent endocytosis. While it is well established that reovirus virions take advantage of clathrin-mediated endocytosis to enter cells, ISVPs do not appear to use this pathway (44). Clathrin-independent endocytic pathways have been described, including caveolar endocytosis and macropinocytosis, and these are now known to play a role in the entry of some viruses (49, 72). To investigate the possibility that reovirus ISVPs enter cells through clathrin-independent endocytosis, we first examined the role of dynamin during internalization of reovirus virions and ISVPs. Dynamin, which is involved in the scission of clathrin-coated vesicles and caveolae from the plasma membrane, can be inhibited with the small-molecule inhibitor dynasore (20, 42, 82, 88). We used confocal microscopy to visualize reovirus particle uptake in A549 respiratory epithelial cells that had been pretreated with either vehicle (DMSO) or 100 μM dynasore and then synchronously infected with either T1L virions or ISVPs. This cell line was selected because it is permissive to infection by both virions and ISVPs (24) and it has properties in

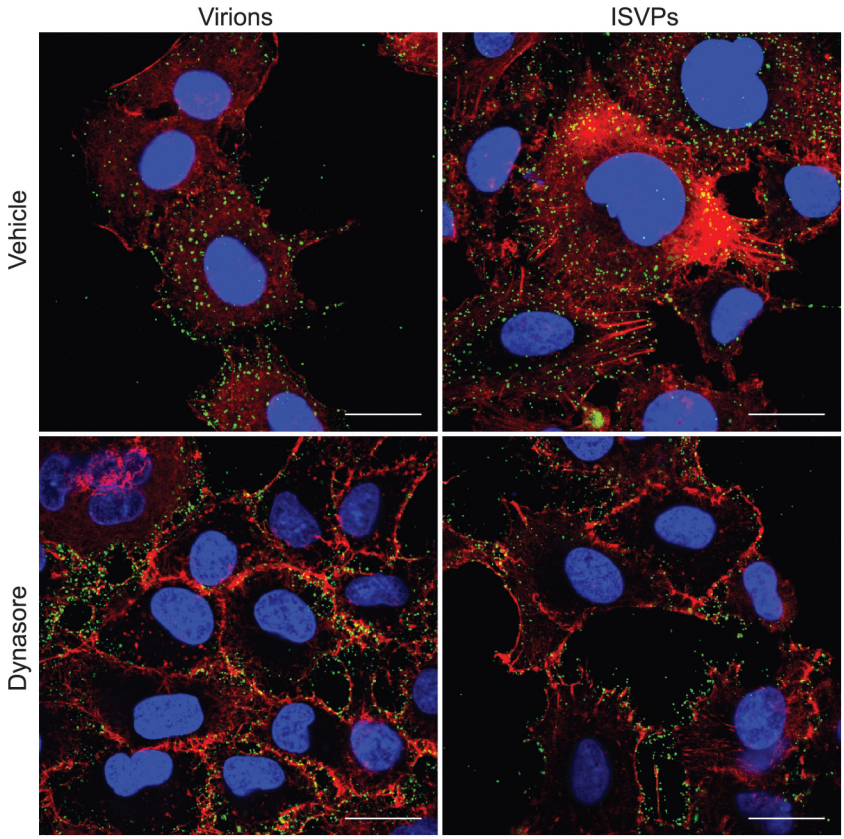

FIG 1 Reovirus virions and ISVPs undergo dynamin-mediated endocytosis. Reovirus T1L virions or ISVPs were adsorbed at a concentration of 1×10^5 particles/cell to adherent A549 cells that had been pretreated with vehicle (DMSO) or dynasore. The monolayers were fixed at 10 min postinfection and labeled with anti-reovirus T1L antiserum (green), phalloidin (red), and DAPI (blue). Scale bars represent 20 μM.

adherent cell culture that made it easy to visualize particle uptake. Whereas vehicle-treated cells showed significant uptake of virions and ISVPs into the cytoplasm at 10 mpi, we found that particles were concentrated at the periphery of dynasore-treated cells (Fig. 1). The effect of dynasore on virion uptake is consistent with the role of dynamin in clathrin-mediated endocytosis, but the effect on ISVP internalization suggested that these uncoated particles also use a dynamin-dependent endocytic pathway to gain access to the cytoplasm.

Dynasore inhibits infection by ISVPs. The imaging experiments described above suggest that dynamin is required for the entry of ISVPs. However, this approach does not distinguish between infectious and noninfectious particles. To determine if dynamin is important for productive infection, we assessed the growth of ISVPs in the presence of dynasore. L929 cells treated with either DMSO or dynasore were infected with virions or ISVPs at an MOI of 3. Infections were terminated at various times, and viral yields were quantified by plaque assay on L929 cells. We found that dynasore treatment inhibited the growth of both virions (Fig. 2A) and ISVPs (Fig. 2B). Similar results were obtained from human A549 respiratory epithelial cells (Fig. 2C) and human embryonic kidney (HEK) 293 cells (Fig. 2D). These data suggest that ISVPs take advantage of a dynamin-dependent endocytic pathway to infect L929 mouse fibroblasts and transformed human cell lines.

The results of our imaging experiments suggest that dynasore inhibits replication by inhibiting viral uptake; however, they do not rule out another effect on later steps in the replication cycle. To address this possibility, we performed a delayed-addition experiment in which dynasore was added at various times prior to or after adsorption. Cells were harvested at 24 hpi, and infection was analyzed by immunoblotting for the reovirus nonstructural protein μNS. In cultures pretreated with dynasore, infection was inhibited by 90% (Fig. 2E). In contrast, addition of dynasore after adsorption had a minimal effect on viral replication. This finding supports the conclusion drawn from our imaging studies, i.e., that dynasore inhibits reovirus replication at an early step of the viral life cycle.

Agents that disrupt vesicular transport can alter receptor recycling to the cell surface (19). To determine if the inhibitory effect of dynasore on reovirus infection was due to effects on virion attachment, we directly assessed the consequences of treatment on reovirus binding to L929 cells. Cells were pretreated with DMSO or dynasore, and virions were adsorbed for 1 h. The samples were then fixed and stained for reovirus, and binding was analyzed by flow cytometry. We found that vehicle- and dynasore-treated cells had similar fluorescence profiles after reovirus adsorption (Fig. 3A), demonstrating that dynasore treatment does not result in reduced viral binding at the cell surface.

Our results suggested that, like virions, ISVPs enter cells through a dynamin-dependent pathway. To confirm that our working concentration of dynasore inhibited both of the known dynamin-dependent

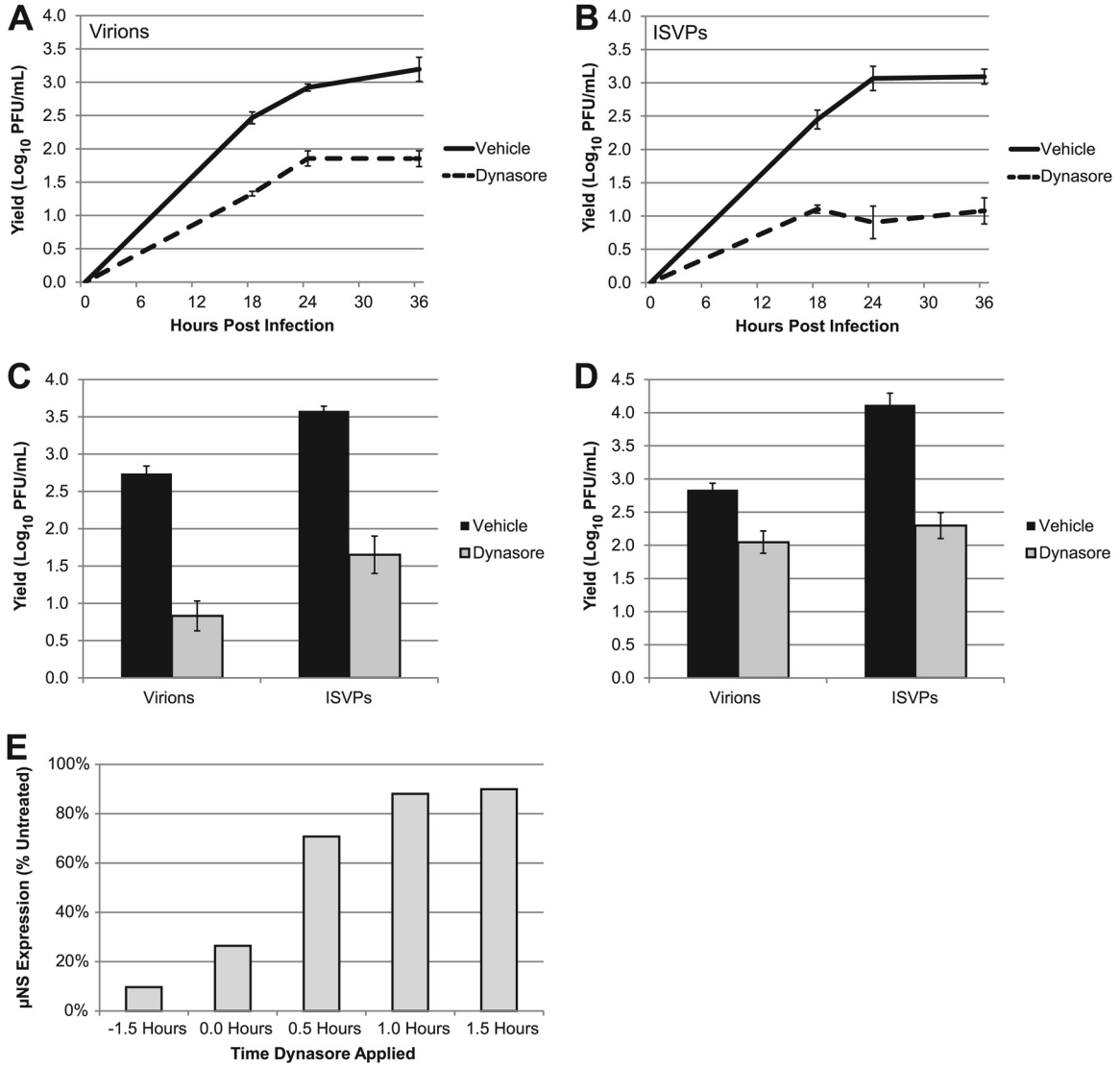

FIG 2 Dynamin plays a role in productive infection by reovirus virions and ISVPs. (A and B) L929 cells were pretreated with vehicle (DMSO) or dynasore and infected with reovirus T1L virions (A) or ISVPs (B) at an MOI of 3. After adsorption, fresh medium with vehicle or inhibitor was added to the cultures, and samples were collected at the indicated times postinfection. Viral yields were quantified by plaque assay on L929 cells. A549 (C) and 293 cells (D) were pretreated with DMSO or dynasore and infected at an MOI of 3. Samples were harvested at 24 hpi, and viral yields were quantified by plaque assay on L929 cells. (E) Dynasore was added to L929 cells at the indicated times prior to or after adsorption with reovirus virions. Infected cell lysates were analyzed at 24 hpi for µNS expression by immunoblotting. Band intensities of µNS and β-actin were quantified to determine the relative µNS expression level of each sample. The values in the graph represent the relative µNS expression level compared to vehicle-treated cells.

pathways, we used the pathway-specific ligands transferrin and cholera toxin subunit B (CTB), which are taken up by clathrin-mediated and caveolar endocytosis, respectively (31, 65). Following dynasore treatment, A549 cells were incubated with prelabeled ligands and fixed at 10 mpi, and the transferrin- and CTB-positive cells were quantified by immunofluorescence. We found that the number of transferrin- and CTB-positive cells was significantly reduced in treated samples (Fig. 3B), demonstrating that dynasore effectively inhibits both clathrin-mediated and caveolar endocytosis. To confirm that dynasore did not affect reovirus growth as a consequence of cytotoxicity, we determined viral yields in cells that were treated with increasing concentrations of the inhibitor. This analysis revealed that dynasore inhibition of reovirus infection was dose dependent, with a maximum effect that plateaued at a concentration of 100 µM, our working concentration for particle uptake and growth experiments (Fig. 3C). Annexin V and propidium iodide staining revealed that dynasore had only minimal effects on cell viability, with cells remaining over 80% viable at all concentrations tested (Fig. 3C). Together, these results argue that the effect of dynasore on reovirus replication is a consequence of the inhibition of dynamin-dependent pathways rather than a nonspecific, cytotoxic effect of the inhibitor.

Virions and ISVPs can utilize caveolar endocytosis for cell entry. While ISVPs had reduced viral yields in dynasore-treated cells, they can infect cells treated with chlorpromazine, which inhibits clathrin-mediated endocytosis (44). These results led us to predict that ISVPs would enter cells through dynamin-dependent, caveolar endocytosis, which has recently been implicated in the entry of avian reovirus (33). To investigate this possibility, we

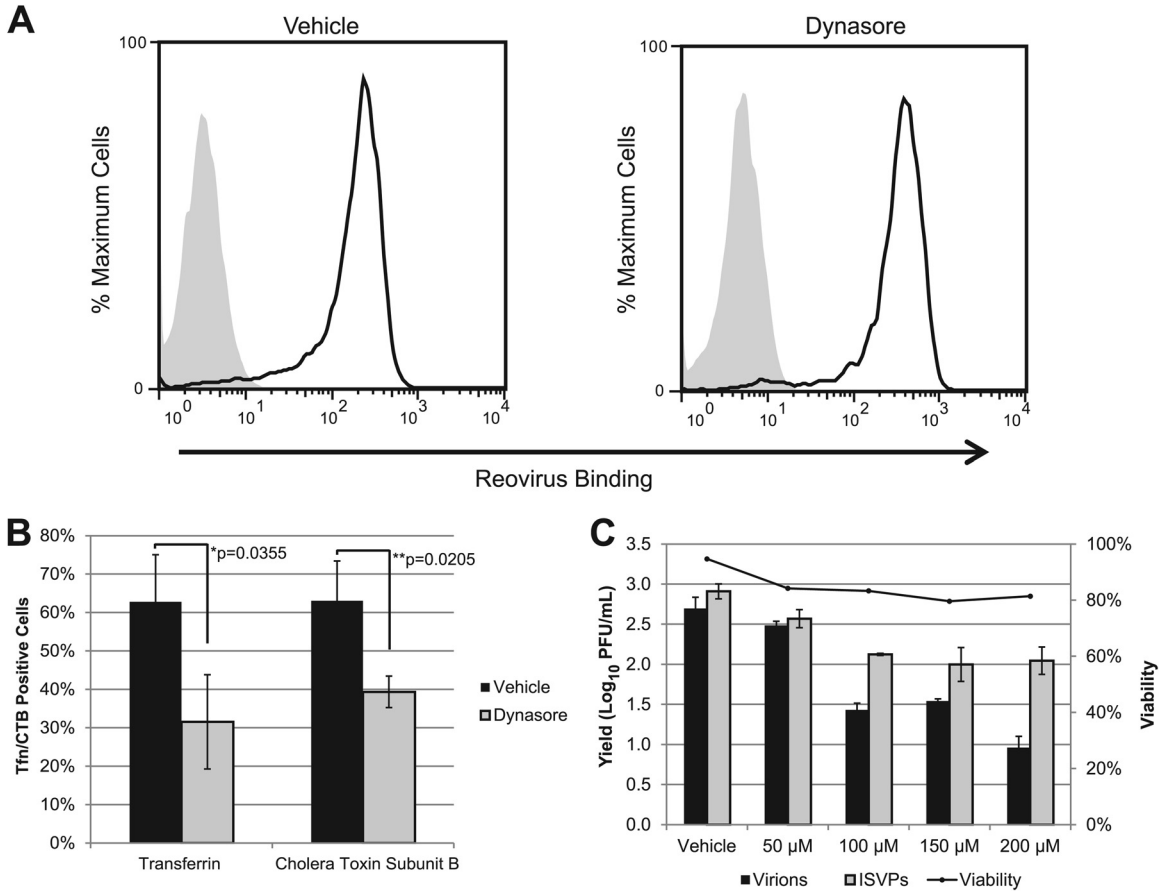

FIG 3 Dynasore inhibits pathway-specific ligand uptake but not reovirus binding or cell viability. (A) L929 cells in suspension culture were pretreated with vehicle (DMSO) or dynasore and adsorbed with reovirus virions at a concentration of 1×10^5 particles/cell (white peaks) or an equivalent volume of gel saline (gray peaks). After adsorption, cells were fixed and stained with an anti-reovirus T1L antibody. Reovirus binding was quantified by flow cytometry. (B) A549 cells were pretreated as described above and then incubated with Alexa 488-transferrin or FITC-CTB. After 1 h at 4°C, warm medium was added to the cultures and the cells were fixed after 30 min. The percentage of transferrin- or CTB-positive cells was determined by counting three similarly confluent fields in three independent experiments. Between 450 and 750 cells were counted in each experiment. Error bars represent standard errors of the means for the three independent experiments. (C) L929 cells were treated with dynasore at the indicated concentrations and incubated for 24 h at 37°C. Cells were stained with annexin V/PI, and viability was assessed by flow cytometry. A parallel set of samples was pretreated with dynasore, infected with T1L virions or ISVPs at an MOI of 3, and assayed for viral yield at 24 hpi.

treated L929 cells with 200 μM genistein to inhibit the caveolar pathway and assessed the effect on viral growth. Consistent with our hypothesis, replication of ISVPs was inhibited by genistein (Fig. 4A). This agent also inhibited the growth of reovirus virions (Fig. 4B), suggesting that these particles are capable of accessing multiple endocytic pathways. Genistein inhibited the replication of both virions and ISVPs in A549 and HEK-293 cells (Fig. 4C), and immunofluorescence analysis revealed that it inhibited particle uptake in A549 cells (W. S. Schulz and L. A. Schiff, unpublished observations). Consistent with published data (45), it inhibited infection by virions but not ISVPs in HeLa cells (Fig. 4D).

Genistein blocks caveolar endocytosis by inhibiting the Src kinase-dependent phosphorylation of caveolin-1, preventing vesicle fusion (5, 60). However, this tyrosine kinase inhibitor can affect other intracellular signal transduction pathways, including those involved in cell cycle progression and apoptosis (36, 58, 64). We assessed the viability of genistein-treated L929 cells to determine if cell death was a factor in reducing viral yields. We found that after 24 h of treatment, genistein did not significantly affect L929 cell viability at any of the concentrations tested but did significantly reduce viral yield (Fig. 4E), arguing against an apoptotic mechanism. We also confirmed that genistein selectively inhibited caveolar endocytosis by analyzing transferrin and CTB uptake in A549 cells. Whereas genistein inhibited CTB internalization, which is caveolin dependent, it had no effect on the clathrin-dependent uptake of transferrin (Fig. 4F). To determine whether genistein targets an early stage in infection, we performed a delayed-addition experiment. In infected cells that were pretreated with genistein, μNS expression was decreased by over 60% (Fig. 4G). However, when genistein was added at or after adsorption, this effect was greatly diminished. This result is consistent with findings for HeLa cells (45) and suggests that genistein inhibits reovirus infection at an early step of the viral life cycle, most likely cell entry.

Caveolin-1 is important for infection by reovirus virions and ISVPs. Because genistein is a broad-spectrum receptor tyrosine kinase inhibitor, we used an independent approach to determine if reovirus particles enter cells through the caveolar pathway.

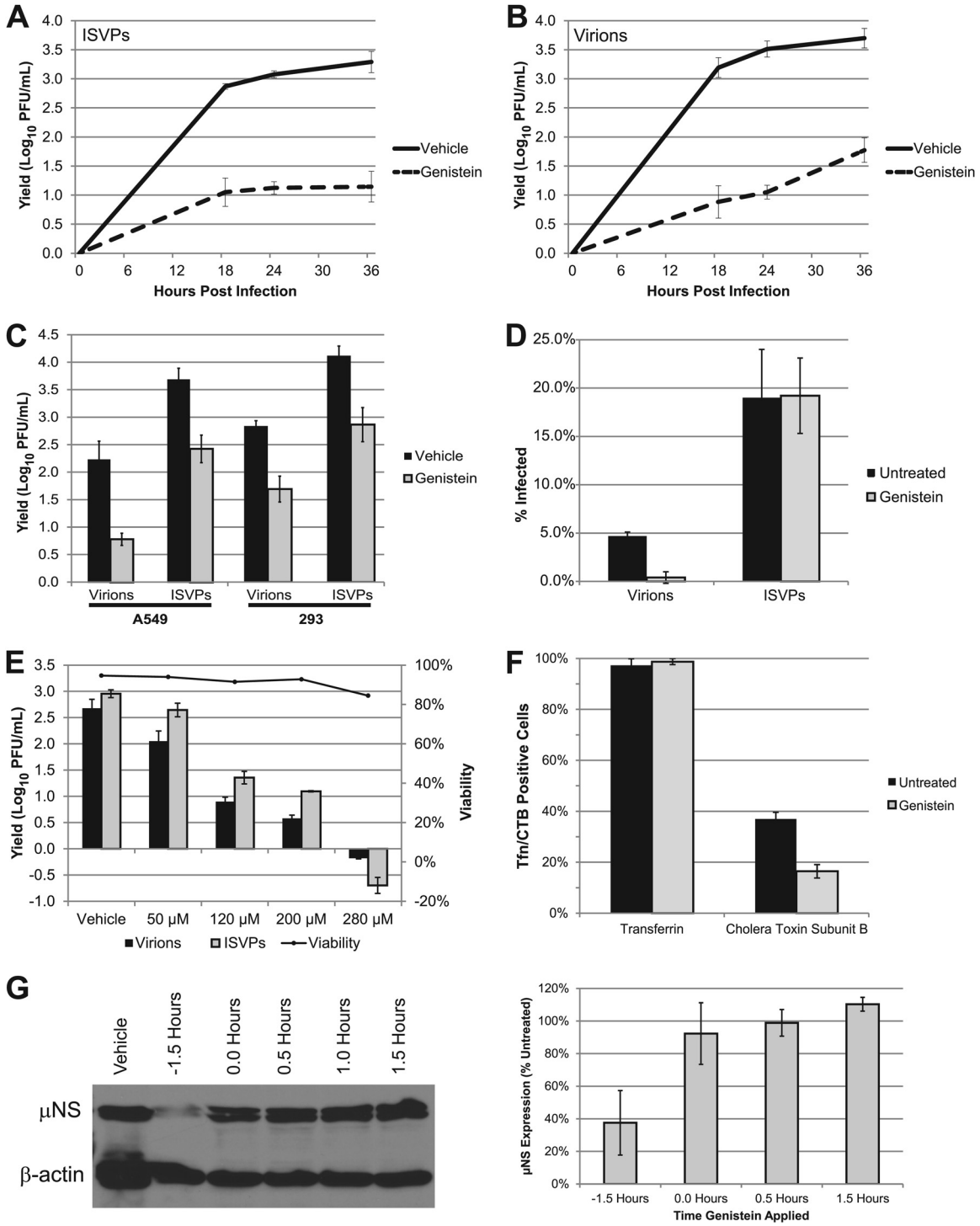

FIG 4 Caveolar endocytosis is important for infection by reovirus virions and ISVPs. (A and B) L929 cells were pretreated with vehicle (DMSO) or 200 μM genistein and infected with reovirus T1L ISVPs (A) or virions (B) at an MOI of 3. Viral yields were determined at the indicated times postinfection by plaque assay on L929 cells. (C) A549 and 293 cells were pretreated and infected as described above, and viral yields were determined at 24 hpi. (D) HeLa cells seeded in 8-well CultureSlides were pretreated as described above and infected at an MOI of 15. At 24 hpi, cultures were fixed and stained with antiserum specific for reovirus T1L. Infection was analyzed by indirect immunofluorescence, and the percentage of infected cells was determined from three equally confluent fields of view. (E) L929 cells were pretreated with the indicated concentrations of genistein, and viability was assessed by annexin V/PI staining at 24 hpi. A parallel set of samples was infected with T1L virions or ISVPs and assayed for viral yield at 24 hpi. (F) A549 cells were pretreated as described above and incubated with Alexa 488-transferrin or FITC-CTB. After 1 h at 4°C, warm medium was added to the cultures and the cells were fixed after 30 min. The percentage of transferrin- or CTB-positive cells was determined by counting three similarly confluent fields. Error bars represent the standard deviations for each sample. (G) Genistein was added to L929 cells at the indicated times prior to or after adsorption with reovirus virions. Infected cell lysates were analyzed at 24 hpi for μNS expression by immunoblotting. The immunoblot (left) is from a representative experiment. Band intensities of μNS and β-actin were quantified to determine the relative μNS expression level of each sample. The values in the graph are derived from three independent experiments and represent the relative μNS expression level compared to that in vehicle-treated cells (right).

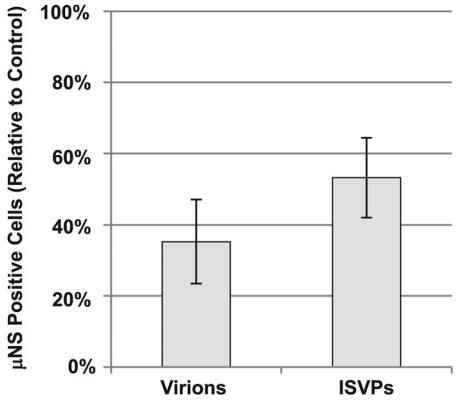

FIG 5 Caveolin-1 is important for infection by virions and ISVPs. 293 cells were transfected with empty vector or vector expressing dominant-negative caveolin-1. Cells were infected with T1L virions or ISVPs 24 h after transfection and then fixed and stained for μNS at 24 hpi. The number of transfected cells that were also μNS positive (infected) was determined by flow cytometry. The relative percentage of infected cells compared to empty vector (pEGFP-N1)-transfected controls is displayed. Error bars represent the standard errors of the means from three independent experiments.

Caveolin-1 is a scaffolding protein involved in caveolar morphogenesis (19). Expression of a dominant-negative form of the protein with a Y14F mutation has been shown to inhibit caveolar endocytosis (5, 25, 59). We transfected HEK-293 cells with either empty vector (pEGFP-N1) or vector expressing dominant-negative caveolin-1 (DN-cav1). Twenty-four hours after transfection, the cultures were infected with either virions or ISVPs. At 24 hpi, infected cultures were fixed and stained with an antiserum directed against the reovirus nonstructural protein μNS, and reovirus-positive cells were quantified by flow cytometry. The percentage of GFP-positive (transfected) cells that were also μNS positive (infected) was calculated for both DN-cav1- and pEGFP-N1-transfected samples in three independent experiments (Fig. 5). This analysis revealed that expression of DN-cav1 significantly reduced infection by reovirus virions and ISVPs relative to the vector-only control. This level of inhibition was similar to that seen with dominant-negative Rab proteins (46). Together, these results support a role for caveolin-1 and caveolar endocytosis during infection by both virions and ISVPs.

Cholesterol is important for infection by reovirus virions. Recent work reveals that many viruses enter cells through specialized, detergent-resistant microdomains of the cell membrane, called lipid rafts (13, 21, 35, 52). To determine if lipid rafts play a role in reovirus infection, we used MβCD to extract membrane cholesterol. Since MβCD can often be cytotoxic, we first assessed viability and viral growth in L929 cells treated with various concentrations of inhibitor. We found that MβCD was cytotoxic at concentrations above 5 mM (Fig. 6A). While the growth of reovirus virions was inhibited at this concentration, the replication of ISVPs was unaffected (Fig. 6A). To determine if the replication of ISVPs was inhibited at later times of infection in MβCD-treated cells, we performed a kinetic analysis. We found that the growth of ISVPs was similar in MβCD- and vehicle-treated cells at each time point tested, while the growth of virions was inhibited (Fig. 6B and C). We examined reovirus binding in the presence of MβCD to determine if cholesterol depletion had a differential effect on the capacity of virions and ISVPs to interact with cells. Reovirus virions or ISVPs were adsorbed to L929 cells that had been pretreated with either vehicle (water) or MβCD to deplete cholesterol. After adsorption, the samples were fixed and stained with anti-reovirus antiserum and binding was analyzed by flow cytometry. We found no difference in the capacity of virions or ISVPs to bind to MβCD-treated samples (Fig. 6D). This finding argues that the growth defect seen after infection with virions is not due to decreased binding by these particles.

Cholesterol can play a critical role in viral assembly as well as viral entry (29). To determine if MβCD affects an early or late event in reovirus infection, we took advantage of the fact that its effect can be reversed by replenishing cholesterol after extraction (57). L929 cells were pretreated with vehicle or MβCD for 1.5 h prior to virus adsorption and cholesterol was added to selected samples, either at the time of adsorption or 30 min prior to adsorption. Viral protein expression was assessed at 24 hpi (Fig. 6E). As expected, viral protein expression was significantly inhibited in MβCD-treated cells that did not receive additional cholesterol. When cholesterol was added to the cultures at the time of virus adsorption, we saw a similarly low level of viral gene expression, but the inhibitory effect of MβCD was diminished when cholesterol was added to the cultures 30 min prior to adsorption, consistent with an effect on early events of infection. Cholesterol depletion has been reported to affect multiple endocytic pathways (51, 66). To better understand the role of cholesterol in reovirus replication, we tested whether MβCD inhibited either of the classical dynamin-dependent pathways under our infection conditions. We found that MβCD treatment did not affect the uptake of either transferrin (Fig. 6F) or CTB (Fig. 6G) in A549 cells, suggesting that it inhibits the replication of reovirus virions by affecting a cholesterol-dependent, dynamin-independent pathway.

We considered the possibility that cholesterol is more important for infections by virions than ISVPs because it plays a direct role in the conversion of virions to ISVPs. To determine if cholesterol promotes ISVP formation, reovirus virions were incubated with cholesterol, chymotrypsin, or both at 32°C. At the indicated times, PMSF was added to inhibit chymotrypsin and particles were visualized by SDS-PAGE. We found that cholesterol had no effect on the formation of ISVPs *in vitro*, as proteolytic cleavage of the μ1c protein to the δ fragment was not altered in the presence of cholesterol, and cholesterol alone did not promote ISVP formation (Fig. 6H). Together, these results are consistent with a model in which cholesterol is important for an early, postbinding step in the reovirus life cycle.

DISCUSSION

Early work on reovirus cell entry showed that virion uncoating by endosomal proteases is an essential step of the viral life cycle (77). This same study demonstrated the presence of both virions and ISVPs within endocytic vesicles at early times of infection. Although these particles appeared to be taken up by endocytosis with equivalent efficiency, it was not clear if endocytosis was a productive pathway for infection by ISVPs. Later studies showed that infection by reovirus virions, but not ISVPs, occurred by uptake through clathrin-mediated endocytosis (44) and that ISVPs could cause direct membrane damage (14, 41). These data suggested that ISVPs may be capable of entering the cytoplasm directly at the cell membrane. In this study, we used two independent chemical inhibitors of caveolar endocytosis as well as dominant-negative caveolin to show that inhibition of the dy-

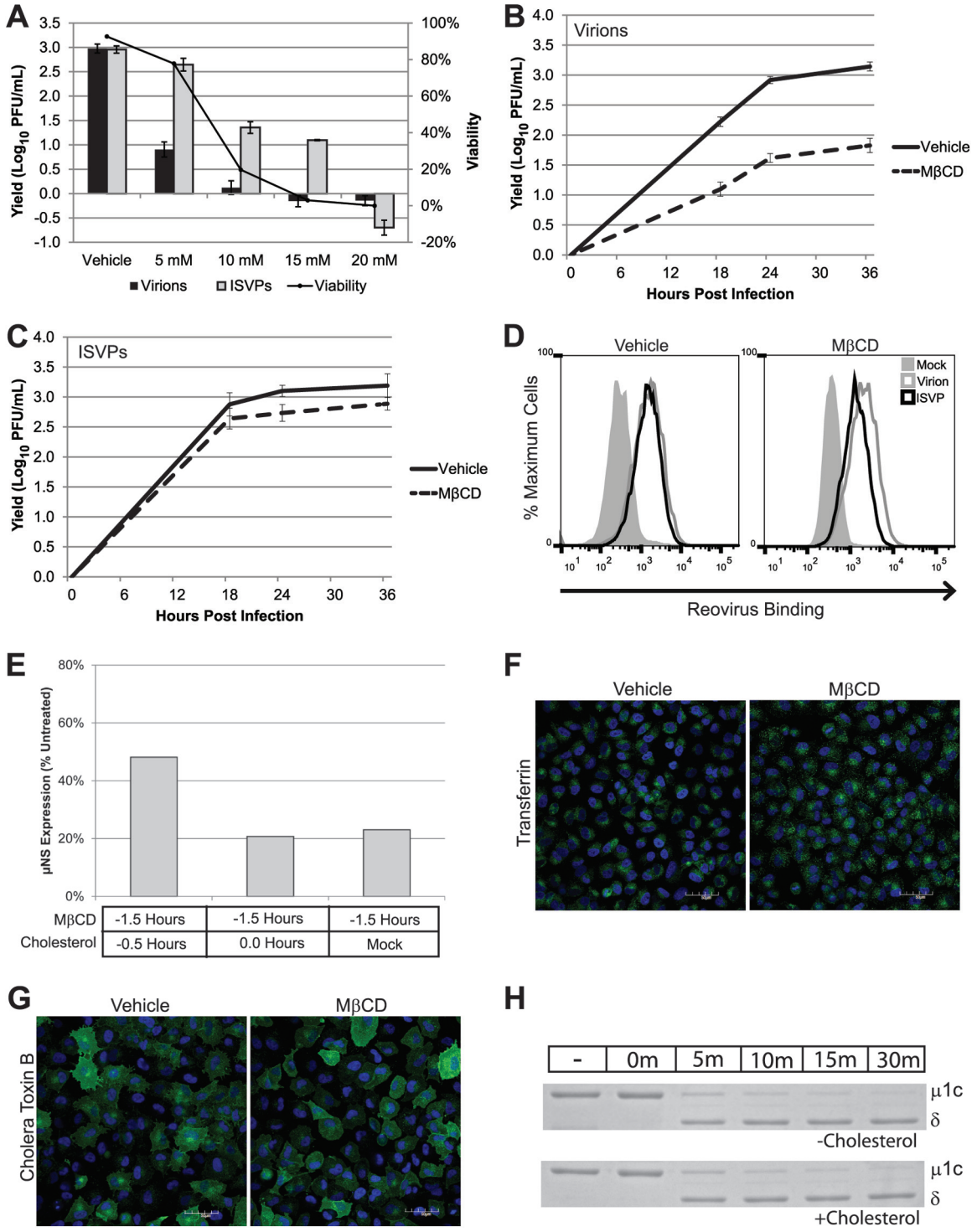

FIG 6 Cholesterol plays a role in infection by reovirus virions. (A) L929 cells were pretreated with the indicated concentrations of MβCD, and viability was assessed at 24 hpi. A parallel set of samples was infected with T1L virions or ISVPs at an MOI of 3 and assayed for viral yield at 24 hpi. (B and C) L929 cells were pretreated with vehicle (water) or 5 mM MβCD and infected with reovirus T1L virions (B) or ISVPs (C) at an MOI of 3. Viral yields were determined at the indicated times postinfection by plaque assay on L929 cells. (D) L929 cells in suspension culture were pretreated with vehicle (water) or MβCD and adsorbed with reovirus virions (gray lines) or ISVPs (black lines) at a concentration of 1×10^5 particles/cell or an equivalent volume of gel saline (shaded peaks). After adsorption, cells were fixed and stained with an anti-reovirus T1L antibody. Reovirus binding was quantified by flow cytometry. (E) Cells were treated with MβCD for 1 h, and 0.1 mM water-soluble cholesterol was added prior to or at the time of adsorption. Infection was analyzed by immunoblotting for μNS at 24 hpi. (F and G) A549 cells were pretreated with vehicle (water) or MβCD for 1 h. Treated cells were incubated with prelabeled transferrin (F) or CTB (G). Warm medium was added to the cultures, and after 15 min cells were fixed and ligand uptake was visualized by confocal microscopy. Scale bars represent 50 μM. (H) Reovirus virions (5×10^{10}) were incubated with chymotrypsin, cholesterol, or both in virion dialysis buffer at 32°C. At the indicated times, digestions were terminated with PMSF and the particles were visualized by SDS-PAGE and Coomassie blue staining.

namin-dependent caveolar pathway significantly reduces yields when infections are initiated with ISVPs.

We found that genistein treatment, which inhibits caveolar endocytosis by preventing vesicle fusion (5, 60), inhibited infection by ISVPs in a number of different cell lines, including L929 mouse fibroblasts, A549 human lung epithelial cells, and 293 human embryonic kidney cells. Dynasore, which inhibits the scission of caveolae, also inhibited ISVP infection in these cells. However, we and others (45) have found that ISVPs are not sensitive to genistein treatment in HeLa cells. Since HeLa cells express very low levels of caveolin (74), this result is not surprising. Reovirus can clearly infect cells that are devoid of caveolae, such as polarized intestinal epithelial cells (7, 56). Because virions are converted to ISVPs in the intestinal tract (8, 9), these data suggest that ISVPs enter intestinal tissue and cells with low levels of caveolar endocytosis through one or more alternative pathways, such as direct membrane penetration or dynamin-independent macropinocytosis, described recently as an entry pathway for Ebola virus (70).

While we have not ruled out direct membrane penetration as an entry mechanism for ISVPs, we have demonstrated that caveolar endocytosis is a route for productive infection by these particles. The function of endocytosis during infection by virions is clear, as uncoating, an essential step in the reovirus life cycle, occurs within the endocytic compartment (78). However, endocytic transport may provide other advantages to reovirus particles during infection, including transport to specific intracellular locations and removal of particles from the cell surface to avoid activation of the immune system (30, 48, 49). Reovirus replication takes place within viral factories located in the perinuclear region of the infected cell (11, 54, 55). Transport of ISVPs to this region is likely important, whether the infection is initiated by uncoated particles or virions that become uncoated in the endocytic pathway. Recent work has shown that reovirus virions need to traffic to late endosomes and that some particles are eventually delivered to lysosomes (46). We detected particles in lysosomes when infections were initiated with either virions or ISVPs (W. S. Schulz and L. A. Schiff, unpublished). This result is consistent with data showing that both clathrin-mediated and caveolar pathways can traffic cargo to lysosomes (26, 28, 61).

Our work suggests that reovirus virions, like adenovirus (4, 85) and influenza virus (17, 67, 73), can enter cells by both dynamin-dependent and dynamin-independent endocytic pathways. Our experiments with pathway-specific ligands argue that multiple dynamin-dependent endocytic pathways and a dynamin-independent pathway function to promote reovirus infection in L929 and A549 cells. In these cell lines, one can demonstrate an effect on viral replication by inhibiting a single pathway; similar results have been reported in other viral systems (23, 40). We showed that MβCD, which extracts membrane cholesterol, inhibits the growth of reovirus virions. Because cholesterol has been implicated in caveolar endocytosis and agents such as MβCD can also affect clathrin-mediated endocytosis at high concentrations (66), we analyzed the uptake of transferrin and cholera toxin subunit B, which depend on the clathrin- and caveolar dynamin-dependent endocytic pathways, respectively. Uptake of these ligands was unaffected by MβCD, which demonstrates that both clathrin-mediated and caveolar pathways are functional and that the requirement for cholesterol in virion entry is not due to effects on clathrin-mediated or caveolar endocytosis. We also found that MβCD treatment had no effect on the binding of reovirus virions or ISVPs to cells and that cholesterol did not promote ISVP formation *in vitro*. These results argue that differences in binding are not responsible for the growth defect seen after virion infection of MβCD-treated cells and that cholesterol is not required for the conversion of virions to ISVPs. Together, these findings suggest that reovirus virions can access a lipid-dependent, dynamin-independent endocytic pathway to establish productive infection. Several such pathways have been described, including macropinocytosis (53) and the clathrin-independent carrier/glycosylphosphatidylinositol-anchored-protein-enriched endosomal compartment (CLIC/GEEC) pathway (38, 69).

Our data demonstrate that reovirus virions and ISVPs use different endocytic pathways for entry. ISVPs enter cells through the caveolar pathway, whereas virions can access clathrin-dependent, caveolar- and dynamin-independent/lipid raft-dependent pathways. These differences may be the consequence of differential exposure of protein motifs on the surface of the two particle types. It has been suggested that exposed Arg-Gly-Asp (RGD) and Lys-Gly-Glu (KGE) motifs on the λ2 protein enable reovirus to recognize β1 integrins (43). Because they are found on a vertex-associated core protein, these motifs would be present on both virions and ISVPs, and their presence cannot explain the differences we found in the entry of virions and ISVPs. Rotavirus, another member of the family *Reoviridae*, engages several integrins for attachment and internalization, including α2β1 and α4β1 (32). We analyzed reovirus capsid sequences for the presence of other potential integrin binding motifs. Our analysis revealed the presence of one such motif (IDSS) in the σ3 protein, which matches the α4β1 binding consensus L/I-D/E-V/S/T-P/S (34, 68). Virion uncoating would lead to the removal of σ3 and the loss of this motif from incoming particles, explaining how virions might activate the clathrin-dependent pathway through integrin binding while ISVPs would not. Reovirus is currently undergoing clinical trials as an oncolytic therapy (47, 76, 80, 81, 86). Many recent trials have examined the efficacy of reovirus as a combination therapy with radiation and chemotherapeutic agents (81). Understanding the cellular pathways used by virions and ISVPs for cell entry is critical to the rational design of combination therapies, because agents that affect critical entry pathways may reduce the efficiency of reovirus as an oncolytic agent. For example, the epidermal growth factor receptor (EGFR) is a target of several chemotherapeutics (63). Inhibition of this receptor reduces caveolin-1 expression (1) and, interestingly, EGFR inhibition can also negatively affect reovirus replication in cell culture (77). Thus, chemotherapeutic agents that target the EGFR might inhibit reovirus entry and infection in patients undergoing combination therapy. As entry is a critical determinant of reovirus oncolysis (2), learning how virions and ISVPs gain access to the cytoplasm is important for the continued development of reovirus as a human cancer treatment.

ACKNOWLEDGMENTS

We thank Linse Lahti, Carol Wells, and Aaron Barnes for technical support. We also thank Max Nibert and Barbara Sherry for their gifts of μNS- and reovirus-specific antisera and Mark McNiven for providing the plasmid expressing dominant-negative caveolin-1. Flow cytometry was conducted at the University of Minnesota Flow Cytometry Core, supported in part by P30 CA77598. Confocal microscopy was completed at the University of Minnesota Imaging Center. We are grateful to Rachel Nygaard, Linse Lahti, and Stephen Rice for providing critical reviews of the manuscript.

This work was supported by Public Health Service grant AI-045990

(L.S.) and by MSTP grant T32 GM008244 (W.S.) from the National Institutes of Health.

REFERENCES

1. **Abulrob A, et al.** 2004. Interactions of EGFR and caveolin-1 in human glioblastoma cells: evidence that tyrosine phosphorylation regulates EGFR association with caveolae. Oncogene **23**:6967–6979.
2. **Alain T, et al.** 2007. Proteolytic disassembly is a critical determinant for reovirus oncolysis. Mol. Ther. **15**:1512–1521.
3. **Amerongen HM, Wilson GA, Fields BN, Neutra MR.** 1994. Proteolytic processing of reovirus is required for adherence to intestinal M cells. J. Virol. **68**:8428–8432.
4. **Amstutz B, et al.** 2008. Subversion of CtBP1-controlled macropinocytosis by human adenovirus serotype 3. EMBO J. **27**:956–969.
5. **Aoki T, Nomura R, Fujimoto T.** 1999. Tyrosine phosphorylation of caveolin-1 in the endothelium. Exp. Cell Res. **253**:629–636.
6. **Barton ES, Chappell JD, Connolly JL, Forrest JC, Dermody TS.** 2001. Reovirus receptors and apoptosis. Virology **290**:173–180.
7. **Barton ES, et al.** 2001. Junction adhesion molecule is a receptor for reovirus. Cell **104**:441–451.
8. **Bass DM, et al.** 1990. Intraluminal proteolytic activation plays an important role in replication of type 1 reovirus in the intestines of neonatal mice. J. Virol. **64**:1830–1833.
9. **Bodkin DK, Nibert ML, Fields BN.** 1989. Proteolytic digestion of reovirus in the intestinal lumens of neonatal mice. J. Virol. **63**:4676–4681.
10. **Borsa J, Copps TP, Sargent MD, Long DG, Chapman JD.** 1973. New intermediate subviral particles in the in vitro uncoating of reovirus virions by chymotrypsin. J. Virol. **11**:552–564.
11. **Broering TJ, et al.** 2004. Reovirus nonstructural protein mu NS recruits viral core surface proteins and entering core particles to factory-like inclusions. J. Virol. **78**:1882–1892.
12. **Carson SD, Kim K-S, Pirruccello SJ, Tracy S, Chapman NM.** 2007. Endogenous low-level expression of the coxsackievirus and adenovirus receptor enables coxsackievirus B3 infection of RD cells. J. Gen. Virol. **88**:3031–3038.
13. **Carter GC, et al.** 2009. HIV entry in macrophages is dependent on intact lipid rafts. Virology **386**:192–202.
14. **Chandran K, Farsetta DL, Nibert ML.** 2002. Strategy for nonenveloped virus entry: a hydrophobic conformer of the reovirus membrane penetration protein micro 1 mediates membrane disruption. J. Virol. **76**:9920–9933.
15. **Coffey MC, Strong JE, Forsyth PA, Lee PW.** 1998. Reovirus therapy of tumors with activated Ras pathway. Science **282**:1332–1334.
16. **Coyne CB, Kim KS, Bergelson JM.** 2007. Poliovirus entry into human brain microvascular cells requires receptor-induced activation of SHP-2. EMBO J. **26**:4016–4028.
17. **de Vries E, et al.** 2011. Dissection of the influenza A virus endocytic routes reveals macropinocytosis as an alternative entry pathway. PLoS Pathog. **7**:e1001329. doi:10.1371/journal.ppat.1001329.
18. **Diaz F, et al.** 2009. Clathrin adaptor AP1B controls adenovirus infectivity of epithelial cells. Proc. Natl. Acad. Sci. U. S. A. **106**:11143–11148.
19. **Doherty GJ, McMahon HT.** 2009. Mechanisms of endocytosis. Annu. Rev. Biochem. **78**:857–902.
20. **Fish KN, Schmid SL, Damke H.** 2000. Evidence that dynamin-2 functions as a signal-transducing GTPase. J. Cell Biol. **150**:145–154.
21. **Fujioka Y, et al.** 2011. The Ras-PI3K signaling pathway is involved in clathrin-independent endocytosis and the internalization of influenza viruses. PLoS One **6**:e16324. doi:10.1371/journal.pone.0016324.
22. **Furlong DB, Nibert ML, Fields BN.** 1988. Sigma 1 protein of mammalian reoviruses extends from the surfaces of viral particles. J. Virol. **62**:246–256.
23. **Gastaldelli M, et al.** 2008. Infectious adenovirus type 2 transport through early but not late endosomes. Traffic **9**:2265–2278.
24. **Golden JW, Linke J, Schmechel S, Thoemke K, Schiff LA.** 2002. Addition of exogenous protease facilitates reovirus infection in many restrictive cells. J. Virol. **76**:7430–7443.
25. **Grande-GarcíA A, et al.** 2007. Caveolin-1 regulates cell polarization and directional migration through Src kinase and Rho GTPases. J. Cell Biol. **177**:683–694.
26. **Grove J, Marsh M.** 2011. The cell biology of receptor-mediated virus entry. J. Cell Biol. **195**:1071–1082.
27. **Harrison SC.** 2008. Viral membrane fusion. Nat. Struct. Mol. Biol. **15**:690–698.
28. **Hayer A, et al.** 2010. Caveolin-1 is ubiquitinated and targeted to intralumenal vesicles in endolysosomes for degradation. J. Cell Biol. **191**:615–629.
29. **Heaton NS, Randall G.** 2011. Multifaceted roles for lipids in viral infection. Trends Microbiol. **19**:368–375.
30. **Helenius A, Kartenbeck J, Simons K, Fries E.** 1980. On the entry of Semliki forest virus into BHK-21 cells. J. Cell Biol. **84**:404–420.
31. **Henley JR, Krueger EW, Oswald BJ, McNiven MA.** 1998. Dynamin-mediated internalization of caveolae. J. Cell Biol. **141**:85–99.
32. **Hewish MJ, Takada Y, Coulson BS.** 2000. Integrins alpha2beta1 and alpha4beta1 can mediate SA11 rotavirus attachment and entry into cells. J. Virol. **74**:228–236.
33. **Huang WR, et al.** 2011. Cell entry of avian reovirus follows a caveolin-1-mediated and dynamin-2-dependent endocytic pathway that requires activation of p38 mitogen-activated protein kinase (MAPK) and Src signaling pathways as well as microtubules and small GTPase Rab5 protein. J. Biol. Chem. **286**:30780–30794.
34. **Humphries JD, Byron A, Humphries MJ.** 2006. Integrin ligands at a glance. J. Cell Sci. **119**:3901–3903.
35. **Imelli N, Meier O, Boucke K, Hemmi S, Greber UF.** 2004. Cholesterol is required for endocytosis and endosomal escape of adenovirus type 2. J. Virol. **78**:3089–3098.
36. **Ismail IA, Kang K-S, Lee HA, Kim J-W, Sohn Y-K.** 2007. Genistein-induced neuronal apoptosis and G_2/M cell cycle arrest is associated with MDC1 up-regulation and PLK1 down-regulation. Eur. J. Pharmacol. **575**:12–20.
37. **Joklik WK.** 1972. Studies on the effect of chymotrypsin on reovirions. Virology **49**:700–715.
38. **Kirkham M, et al.** 2005. Ultrastructural identification of uncoated caveolin-independent early endocytic vehicles. J. Cell Biol. **168**:465–476.
39. **Lee PW, Hayes EC, Joklik WK.** 1981. Protein sigma 1 is the reovirus cell attachment protein. Virology **108**:156–163.
40. **Li E, et al.** 2000. Association of p130CAS with phosphatidylinositol-3-OH kinase mediates adenovirus cell entry. J. Biol. Chem. **275**:14729–14735.
41. **Lucia-Jandris P, Hooper JW, Fields BN.** 1993. Reovirus M2 gene is associated with chromium release from mouse L cells. J. Virol. **67**:5339–5345.
42. **Macia E, et al.** 2006. Dynasore, a cell-permeable inhibitor of dynamin. Dev. Cell **10**:839–850.
43. **Maginnis MS, et al.** 2006. Beta1 integrin mediates internalization of mammalian reovirus. J. Virol. **80**:2760–2770.
44. **Maginnis MS, et al.** 2008. NPXY motifs in the beta1 integrin cytoplasmic tail are required for functional reovirus entry. J. Virol. **82**:3181–3191.
45. **Mainou BA, Dermody TS.** 2011. Src kinase mediates productive endocytic sorting of reovirus during cell entry. J. Virol. **85**:3203–3213.
46. **Mainou BA, Dermody TS.** 2012. Transport to late endosomes is required for efficient reovirus infection. J. Virol. **86**:8346–8358.
47. **Marcato P, Shmulevitz M, Lee PW.** 2005. Connecting reovirus oncolysis and Ras signaling. Cell Cycle. **4**:556–559.
48. **Marsh M, Bron R.** 1997. SFV infection in CHO cells: cell-type specific restrictions to productive virus entry at the cell surface. J. Cell Sci. **110**:95–103.
49. **Marsh M, Helenius A.** 2006. Virus entry: open sesame. Cell **124**:729–740.
50. **Mason SD, Joyce J.** 2011. Proteolytic networks in cancer. Trends Cell Biol. **21**:228–237.
51. **Mayor S, Pagano RE.** 2007. Pathways of clathrin-independent endocytosis. Nat. Rev. Mol. Cell Biol. **8**:603–612.
52. **Meier O, et al.** 2002. Adenovirus triggers macropinocytosis and endosomal leakage together with its clathrin-mediated uptake. J. Cell Biol. **158**:1119–1131.
53. **Mercer J, Helenius A.** 2008. Vaccinia virus uses macropinocytosis and apoptotic mimicry to enter host cells. Science **320**:531–535.
54. **Miller CL, Arnold MM, Broering TJ, Hastings CE, Nibert ML.** 2010. Localization of mammalian orthoreovirus proteins to cytoplasmic factory-like structures via nonoverlapping regions of microNS. J. Virol. **84**:867–882.
55. **Miller CL, Broering TJ, Parker JSL, Arnold MM, Nibert ML.** 2003. Reovirus sigma NS protein localizes to inclusions through an association requiring the mu NS amino terminus. J. Virol. **77**:4566–4576.
56. **Mirre C, Monlauzeur L, Garcia M, Delgrossi MH, Le Bivic A.** 1996.

Detergent-resistant membrane microdomains from Caco-2 cells do not contain caveolin. Am. J. Physiol. **271**:C887—C894.
57. **Ostrom RS, Liu X.** 2007. Detergent and detergent-free methods to define lipid rafts and caveolae. Methods Mol. Biol. **400**:459–468.
58. **Ouyang G, et al.** 2009. Genistein induces G_2/M cell cycle arrest and apoptosis of human ovarian cancer cells via activation of DNA damage checkpoint pathways. Cell Biol. Int. **33**:1237–1244.
59. **Parton RG.** 1996. Caveolae and caveolins. Curr. Opin. Cell Biol. **8**:542–548.
60. **Parton RG, Joggerst B, Simons K.** 1994. Regulated internalization of caveolae. J. Cell Biol. **127**:1199–1215.
61. **Parton RG, Howes MT.** 2010. Revisiting caveolin trafficking: the end of the caveosome. J. Cell Biol. **191**:439–441.
62. **Patel KP, Coyne CB, Bergelson JM.** 2009. Dynamin- and lipid Raft-dependent entry of decay-accelerating factor (DAF)-binding and non-DAF-binding coxsackieviruses into nonpolarized cells. J. Virol. **83**:11064–11077.
63. **Petrelli F, Borgonovo K, Cabiddu M, Barni S.** 2012. Efficacy of EGFR tyrosine kinase inhibitors in patients with EGFR-mutated non-small-cell lung cancer: a meta-analysis of 13 randomized trials. Clin. Lung Cancer **13**:107–114.
64. **Ramos S.** 2007. Effects of dietary flavonoids on apoptotic pathways related to cancer chemoprevention. J. Nutr. Biochem. **18**:427–442.
65. **Reed RA, Mattai J, Shipley GG.** 1987. Interaction of cholera toxin with ganglioside GM1 receptors in supported lipid monolayers. Biochemistry **26**:824–832.
66. **Rodal SK, et al.** 1999. Extraction of cholesterol with methyl-beta-cyclodextrin perturbs formation of clathrin-coated endocytic vesicles. Mol. Biol. Cell **10**:961–974.
67. **Roy AM, Parker JS, Parrish CR, Whittaker GR.** 2000. Early stages of influenza virus entry into Mv-1 lung cells: involvement of dynamin. Virology **267**:17–28.
68. **Ruoslahti E.** 1996. RGD and other recognition sequences for integrins. Annu. Rev. Cell Dev. Biol. **12**:697–715.
69. **Sabharanjak S, Sharma P, Parton RG, Mayor S.** 2002. GPI-anchored proteins are delivered to recycling endosomes via a distinct cdc42-regulated, clathrin-independent pinocytic pathway. Dev. Cell **2**:411–423.
70. **Saeed MF, Kolokoltsov A, Albrecht T, Davey R.** 2010. Cellular entry of Ebola virus involves uptake by a macropinocytosis-like mechanism and subsequent trafficking through early and late endosomes. PLoS Pathog. **6**:e1001110. doi:10.1371/journal.ppat.1001110.
71. **Shmulevitz M, Marcato P, Lee PWK.** 2005. Unshackling the links between reovirus oncolysis, Ras signaling, translational control and cancer. Oncogene **24**:7720–7728.
72. **Sieczkarski SB, Whittaker GR.** 2002. Dissecting virus entry via endocytosis. J. Gen. Virol. **83**:1535–1545.
73. **Sieczkarski SB, Whittaker GR.** 2002. Influenza virus can enter and infect cells in the absence of clathrin-mediated endocytosis. J. Virol. **76**:10455–10464.
74. **Singh RD, et al.** 2003. Selective caveolin-1-dependent endocytosis of glycosphingolipids. Mol. Biol. Cell **14**:3254–3265.
75. **Sloane BF, et al.** 2005. Cathepsin B and tumor proteolysis: contribution of the tumor microenvironment. Semin. Cancer Biol. **15**:149–157.
76. **Strong JE, Coffey MC, Tang D, Sabinin P, Lee PW.** 1998. The molecular basis of viral oncolysis: usurpation of the Ras signaling pathway by reovirus. EMBO J. **17**:3351–3362.
77. **Strong JE, Lee PW.** 1996. The v-erbB oncogene confers enhanced cellular susceptibility to reovirus infection. J. Virol. **70**:612–616.
78. **Sturzenbecker LJ, Nibert M, Furlong D, Fields BN.** 1987. Intracellular digestion of reovirus particles requires a low pH and is an essential step in the viral infectious cycle. J. Virol. **61**:2351–2361.
79. **Tai JH, et al.** 2005. Prevalence of reovirus-specific antibodies in young children in Nashville, Tennessee. J. Infect. Dis. **191**:1221–1224.
80. **Thirukkumaran CM, et al.** 2010. Oncolytic viral therapy for prostate cancer: efficacy of reovirus as a biological therapeutic. Cancer Res. **70**:2435–2444.
81. **Thirukkumaran C, Morris DG.** 2009. Oncolytic viral therapy using reovirus. Methods Mol. Biol. **542**:607–634.
82. **Thompson HM, McNiven M.** 2006. Discovery of a new "dynasore." Nat. Chem. Biol. **2**:355–356.
83. **Tsai B.** 2007. Penetration of nonenveloped viruses into the cytoplasm. Annu. Rev. Cell Dev. Biol. **23**:23–43.
84. **Virgin HW, Bassel-Duby R, Fields BN, Tyler KL.** 1988. Antibody protects against lethal infection with the neurally spreading reovirus type 3 (Dearing). J. Virol. **62**:4594–4604.
85. **Wickham TJ, Mathias P, Cheresh DA, Nemerow GR.** 1993. Integrins alpha v beta 3 and alpha v beta 5 promote adenovirus internalization but not virus attachment. Cell **73**:309–319.
86. **Wilcox ME, et al.** 2001. Reovirus as an oncolytic agent against experimental human malignant gliomas. J. Natl. Cancer Inst. **93**:903–912.
87. **Yang Y, et al.** 2010. Cathepsin S mediates gastric cancer cell migration and invasion via a putative network of metastasis-associated proteins. J. Proteome Res. **9**:4767–4778.
88. **Yao Q, et al.** 2005. Caveolin-1 interacts directly with dynamin-2. J. Mol. Biol. **348**:491–501.
89. **Zhang L, et al.** 2009. Requirements for the formation of membrane pores by the reovirus myristoylated micro1N peptide. J. Virol. **83**:7004–7014.